arXiv:1402.7188v1 [hep-ph] 28 Feb 2014

March 3, 2014
MISC-2014-02

Effects to $\sin\theta_{12}$ from perturbation of the neutrino mixing matrix with the partially degenerated neutrino masses

Takeshi Araki[a1], Eiichi Takasugi[a,b2],

[a)] *Maskawa Institute, Kyoto Sangyo University, Kita-Ku, Kyoto 603-8555, Japan*
[b)] *Department of Physics, Osaka University, Toyonaka, Osaka 560-0043, Japan*

Abstract

We consider a situation where the leading-order neutrino mass matrix is derived by the theoretical ansatz and reproduces the experimental data well, but not preciously. Then, the next stage is to try to fully reproduce the data by adding small perturbation terms. In this paper, we obtain the analytical method to diagonalize the mass matrix and find a consistency condition that parameters should satisfy not to change $\sin\theta_{12}$ much. This condition could require parameter-tuning and plays a crucial role to relate the added perturbation terms with the prediction analytically, in particular, for the case of the partially-quasi-degenerated neutrino masses ($m_2 \simeq m_1$) where neutrinoless double beta decays would be observed in the phase-Ⅱ experiments.

1 Introduction

Various types of the neutrinoless double beta decay ($0\nu\beta\beta$) experiments have been working, and the phase-Ⅱ experiments are planned; see Refs. [1, 2], [3, 4, 5], and [6, 7] for the recent reviews, studies with cosmological observations, and previous works, respectively. In these experiments, the expected sensitivity to the effective neutrino mass, $\langle m_\nu \rangle$, would hopefully reach to 0.02 eV. As discussed by many authors, if the observed effective mass $\langle m_\nu \rangle$ is in regions much larger than $\sqrt{\Delta m_a^2} \simeq 0.049$ eV, the possible mass pattern is the quasi-degenerate (QD) one (see Fig. 1). If $\langle m_\nu \rangle$ is greater than or equal to 0.049 eV, the inverted hierarchy (IH) with the constructive interference of the Majorana CP phases between m_2 and m_1 would be favored. For the IH case with the destructive interface, $\langle m_\nu \rangle$ is greater than or equal to 0.014 eV. In the case of the normal hierarchy (NH), with the sensitivity of $\langle m_\nu \rangle > 0.02$ eV, one could explore the partially-quasi-degenerated mass regions, in which $m_2 \simeq m_1$; especially, most of the constructive interference regions would be covered. Thus, these parameter regions are expected to be important in the coming years.

Let us suppose that the leading-order neutrino mass matrix M_0 is derived theoretically with use of some symmetry and that its diagonalizing matrix V_0, which is defined by

$$\overline{M_0} \equiv V_0^T M_0 V_0 = \begin{pmatrix} m_1^0 e^{i\alpha_0} & 0 & 0 \\ 0 & m_2^0 e^{i\beta_0} & 0 \\ 0 & 0 & m_3^0 \end{pmatrix}, \tag{1}$$

reproduces the experimental data of the mixing angles well, but not preciously. In particular, $(V_0)_{12}$ is assumed to be very close to its experimental value. Here, m_i^0 are taken to be real and positive, and β_0 and α_0 are their CP phases. In order to fill the gap between V_0 and the experimental data, we add three small complex parameters:

$$\begin{pmatrix} 0 & \epsilon_1 & \epsilon_3 \\ \epsilon_1 & 0 & \epsilon_2 \\ \epsilon_3 & \epsilon_2 & 0 \end{pmatrix}. \tag{2}$$

[1] E-mail: araki@cc.kyoto-su.ac.jp
[2] E-mail: takasugi.e@gmail.com

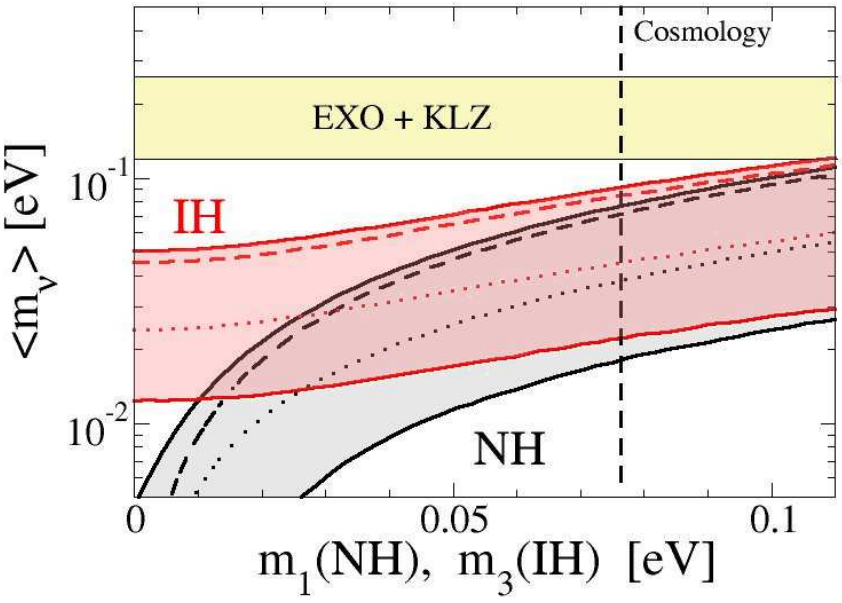

Figure 1: The effective mass, $\langle m_\nu \rangle$, of the $0\nu\beta\beta$ as functions of the lightest neutrino masses, m_1 (m_3) for the NH (IH) case; all the CP phases are varied from 0 to 2π; the gray (red) region is allowed by the 3σ constraints of the oscillation parameters [8] for the NH (IH) case; the upper (lower) regions surrounded by the dashed- (dotted-) and solid-curves are regions of the constructive (destructive) interference of the Majorana phases; the horizontal yellow bound represents the 90% C.L. upper bound on $\langle m_\nu \rangle$ from the combined analysis of the EXO and KamLAND-Zen (KLZ) experiments [9, 10]; the vertical-dashed line corresponds to the 95% C.L. upper bound on the sum of the neutrino masses from the Planck and other cosmological observations [11].

In model-building, we put some restriction on the parameters ϵ_i and obtain prediction. Our question is to see analytically the relation between the restriction and the prediction. For this, we have to diagonalize the neutrino mass matrix analytically as precisely as possible and then expand the exact result in terms of small parameters. We develop a powerful method to achieve this and see the relation between the restriction and the prediction. In the course of this, we find a constraint which parameters should satisfy in order not to change $\sin\theta_{12}$ much. This is the condition for the model to be consistent. In view of the observability in the future $0\nu\beta\beta$ experiments, we are mainly interested in the partially-quasi-degenerated mass regions and pay special attention to three cases: the NH with the constructive interference case and the IH[3] with the constructive and destructive interference cases. Nevertheless, we sometimes consider the other cases for the sake of completeness.

In Sect. 2, we review the behavior of the effective mass of the $0\nu\beta\beta$ with respect to $p = m_2/m_3$ and the Majorana phases [12, 13] for the purpose of the following sections. In Sect. 3, the diagonalization of a symmetric matrix with small perturbation terms is developed, and then the consistency condition which guarantees that $\sin\theta_{12}$ does not change much is derived in Sect. 4. In Sect. 5, the developed method is applied to the case of the tri-bi-maximal mixing, and the relations between the restriction of parameters and the prediction are given for various models in Sect. 6. The concluding remarks are given in Sect. 7.

[3]In the case of IH, m_2 is always quasi-degenerated with m_1.

2 Behavior of effective mass of $0\nu\beta\beta$

In the introduction, we argued that our main interests are the NH case for the regions of $m_2 \simeq m_1$ with the constructive interference, and the IH cases with both the constructive and destructive interferences. We here summarize the behavior of $\langle m_\nu \rangle$ for these cases. In the followings, we use the convention that the mass parameter m_i are real and positive and that m_2 and m_1 are accompanied by the Majorana phases β and α, respectively. These Majorana phases appear in the mixing matrix as the phase matrix $P = \mathrm{diag}(e^{-\frac{i}{2}\alpha},\ e^{-\frac{i}{2}\beta},\ 1)$.

Let us define

$$p = \frac{m_2}{m_3} \tag{3}$$

- The NH case for the regions of $m_2 \simeq m_1$ with the constructive interference $\beta \simeq \alpha$
  In this case, $p < 1$ and neutrino masses are expressed as

$$m_2 = \frac{p}{\sqrt{1-p^2}}\sqrt{\Delta m_a^2}, \quad m_3 = \frac{1}{\sqrt{1-p^2}}\sqrt{\Delta m_a^2}. \tag{4}$$

  The effective mass is written by

$$\langle m_\nu \rangle \simeq |(c_{12}c_{13})^2 m_1 e^{i\alpha} + (s_{12}c_{13})^2 m_2 e^{i\beta}| \simeq m_2 = \frac{p}{\sqrt{1-p^2}}\sqrt{\Delta m_a^2}, \tag{5}$$

  where s_{ij} (c_{ij}) stands for $\sin\theta_{ij}$ ($\cos\theta_{ij}$), and we have used $s_{13} \ll 1$. For $\langle m_\nu \rangle > 0.02$eV, one finds $p > 0.4$.

- The IH case
  In this case, $p > 1$ and

$$m_2 = \frac{1}{\sqrt{1-(1/p)^2}}\sqrt{\Delta m_a^2}, \quad m_3 = \frac{(1/p)}{\sqrt{1-(1/p)^2}}\sqrt{\Delta m_a^2}. \tag{6}$$

  On one hand, the effective mass for the destructive interference case is

$$\langle m_\nu \rangle \simeq m_2 |c_{13}\cos 2\theta_{12}| \simeq \frac{|\cos 2\theta_{12}|}{\sqrt{1-(1/p)^2}}\sqrt{\Delta m_a^2} \geq 0.014 \text{ eV}, \tag{7}$$

  for the 3σ upper bound $\sin^2\theta_{12} < 0.359$ [8]. On the other hand, the constructive interference case is

$$\langle m_\nu \rangle \simeq m_2 = \frac{1}{\sqrt{1-1/p^2}}\sqrt{\Delta m_a^2} \geq 0.049 \text{ eV}. \tag{8}$$

3 Diagonalization of symmetric matrix with small perturbation terms

We supplement the leading-order neutrino mass matrix Eq. (1) by the small perturbation terms in Eq. (2) and define the full mass matrix as

$$\overline{M} = \mu \left[\begin{pmatrix} k_1 & 0 & 0 \\ 0 & k_2 & 0 \\ 0 & 0 & k_3 \end{pmatrix} + \begin{pmatrix} 0 & \epsilon_1 & \epsilon_3 \\ \epsilon_1 & 0 & \epsilon_2 \\ \epsilon_3 & \epsilon_2 & 0 \end{pmatrix} \right] = \mu \begin{pmatrix} A & X \\ X^T & k_3 \end{pmatrix}, \tag{9}$$

where

$$A = \begin{pmatrix} k_1 & \epsilon_1 \\ \epsilon_1 & k_2 \end{pmatrix}, \ X = \begin{pmatrix} \epsilon_3 \\ \epsilon_2 \end{pmatrix}, \tag{10}$$

and the overall factor μ stands for the heaviest mass among m_i^0: $\mu = m_3^0$ (m_2^0) for the NH (IH) case. We emphasize that this is the most-general complex symmetric matrix in the sense of the number of parameters. Throughout this paper, we choose a basis in which the charged lepton mass matrix is diagonal and k_3 is real and positive.

We first make $\overline{M}$ block diagonalized by the unitary matrix V_1:

$$V_1 = \begin{pmatrix} u & Y^* \\ -Y'^T & x \end{pmatrix}, \tag{11}$$

where

$$u = \begin{pmatrix} c_3 & 0 \\ -fg^*/c_3 & c_2 \end{pmatrix}, \qquad x = c_3 c_2, \;\; Y = \begin{pmatrix} f \\ g \end{pmatrix}, \;\; Y' = \begin{pmatrix} fc_2 \\ g/c_3 \end{pmatrix}, \tag{12}$$

and

$$c_3 = \sqrt{1-|f|^2}, \;\; c_2 = \sqrt{\frac{1-|f|^2-|g|^2}{1-|f|^2}}. \tag{13}$$

This V_1 mainly affects $\sin\theta_{13}$ and $\sin\theta_{23}$[4] , and ϵ_3 and ϵ_2 are of the orders of f and g, respectively, as we shall see later. After this transformation, we find

$$V_1^T \bar{M} V_1 = \mu \begin{pmatrix} K & N \\ N^T & L \end{pmatrix}, \tag{14}$$

where

$$\begin{aligned} K &= u^T A u - u^T X Y'^T - Y' X^T u + k_3 Y' Y'^T, \\ N &= u^T A Y^* + x u^T X - Y' X^T Y^* - k_3 x Y', \\ L &= k_3 x^2 + x(X^T Y^* + Y^\dagger X) + Y^\dagger A Y^*, \end{aligned} \tag{15}$$

and $m_3 = \mu |L|$. We require the element N vanishes, which leads to

$$u^T X = \frac{1}{x}(k_3 x Y' - u^T A Y^* + Y' X^T Y^*). \tag{16}$$

This identity relates ϵ_i's with f and g, but we postpone showing their expressions till Eq. (24). The 2×2 matrix K is parametrized as

$$K = \begin{pmatrix} a & c \\ c & b \end{pmatrix}, \tag{17}$$

which can be expressed explicitly in terms of ϵ_i's, but it is also postponed to Eq. (26). As we shall see later, $|b| \gg |c|$.

Next, we diagonalize the matrix K by the unitary matrix V_2:

$$V_2 = \begin{pmatrix} \mathcal{C} & \mathcal{S}e^{i\kappa} \\ -\mathcal{S}e^{-i\kappa} & \mathcal{C} \end{pmatrix}, \tag{18}$$

where $\mathcal{C} = \cos\Theta$ and $\mathcal{S} = \sin\Theta$, and V_2 affects θ_{12}. The important point is that $\mathcal{S}$ will be much smaller than f and g, because we assume that $(V_0)_{12}$ is very close to the experimental data. The angle Θ and the phase κ are given by

$$\tan 2\Theta = 2\frac{|a^* c + b c^*|}{|b|^2 - |a|^2}, \quad \kappa = \arg(a^* c + b c^*), \tag{19}$$

[4] We note that there would be other unitary matrices where $(V_1)_{13} = f^*$ and $(V_1)_{23} = g^*$. Here, we choose the one which keeps $(V_0)_{12}$ unchanged after this transformation, i.e., $(V_0 V_1)_{12} \simeq (V_0)_{12}$.

respectively. The eigenvalues are found to be

$$|\lambda_1|^2 = \left(\frac{m_1}{\mu}\right)^2 = \frac{1}{2}\left\{|a|^2 + |b|^2 + 2|c|^2 - \frac{|b|^2 - |a|^2}{\cos 2\Theta}\right\},$$
$$|\lambda_2|^2 = \left(\frac{m_2}{\mu}\right)^2 = \frac{1}{2}\left\{|a|^2 + |b|^2 + 2|c|^2 + \frac{|b|^2 - |a|^2}{\cos 2\Theta}\right\}, \tag{20}$$

where μ is the overall factor defined in Eq. (9), and $m_{1,2}$ are the physical neutrino masses, which are real and positive. From them, the mass splitting between m_2 and m_1 is written as

$$|\lambda_2|^2 - |\lambda_1|^2 = \frac{\Delta m_s^2}{\mu^2} = \frac{|b|^2 - |a|^2}{\cos 2\Theta}, \tag{21}$$

and we find

$$\sin 2\Theta = 2\mu^2 \frac{|a^* c + b c^*|}{\Delta m_s^2}. \tag{22}$$

The neutrino mixing matrix is obtained by $(V_0 V_1 V_2)$ aside from phases of neutrino masses, which are related to the Majorana phases.

Up to now, the analysis is exact. In what follows, we exploit the fact that ϵ_3 and ϵ_2 (thus, f and g) are small and that ϵ_1 is much smaller than them: as we shall show later, ϵ_1 should be of the order of $\epsilon_{2,3}^2$ or much smaller than it. We hereafter omit terms which are higher than f^2, g^2 and terms proportional to $\epsilon_2 f$ and $\epsilon_2 g$. In this case, Eq.(16) is reduces to be

$$X \simeq k_3 Y - A Y^*, \tag{23}$$

yielding

$$f \simeq \frac{1}{k_3^2 - |k_1|^2}\left[k_3\epsilon_3 + k_1\epsilon_3^*\right], \quad g \simeq \frac{1}{k_3^2 - |k_2|^2}\left[k_3\epsilon_2 + k_2\epsilon_2^*\right], \tag{24}$$

or

$$\epsilon_3 \simeq k_3 f - k_1 f^*, \quad \epsilon_2 \simeq k_3 g - k_2 g^*, \tag{25}$$

and the parameters a, b, and c included in K are expressed as

$$\begin{aligned} a &\simeq k_1(1 + |f|^2) - k_3 f^2, \\ b &\simeq k_2(1 + |g|^2) - k_3 g^2, \\ c &\simeq \epsilon_1 - \epsilon_3 g. \end{aligned} \tag{26}$$

Now, we can compute in a good approximation the neutrino mixing matrix $V = (V_0 V_1 V_2)$, once V_0 is given.

4 Consistency conditions

One may think that the mixing angles are only moderately corrected since ϵ's are assumed to be small. However, $\mathcal{S}$ is not necessarily small; rather, it could take an unrealistically-large value. This is because the denominator of Eq. (22) is preciously measured and is very small. In order for the full mixing matrix V being consistent with the experimental data, therefore, one needs to somehow make the numerator sufficiently small, which leads to

$$|a^* c + b c^*| \simeq \frac{\Delta m_s^2}{\mu^2}\,\Theta \simeq 0. \tag{27}$$

We hereafter refer to this requirement as *consistency condition*. In the followings, we further examine it by categorizing the neutrino mass spectrum into three types.

1. The NH case in the regions of $m_2 \gg m_1$.
   In the case of NH, $\mu = m_3^0$ and

$$k_1 = \frac{m_1^0}{m_3^0} e^{i\alpha_0}, \quad k_2 = \frac{m_2^0}{m_3^0} e^{i\beta_0}, \quad k_3 = 1. \tag{28}$$

   With Eq. (26), the left-hand side of Eq. (27) is written by

$$|a^* c + b c^*| \simeq \left| \frac{m_1^0}{m_3^0} e^{-i\alpha_0} (\epsilon_1 - \epsilon_3 g) + \frac{m_2^0}{m_3^0} e^{i\beta_0} (\epsilon_1 - \epsilon_3 g)^* \right|. \tag{29}$$

   Note that m_i^0 are taken to be real and positive, and g is given in Eq. (24). Since $m_2 \simeq m_2^0$ and $m_2 \gg m_1$, the term proportional to m_1^0 may be dropped in comparison with that of m_2^0. By using the approximations $m_3^0 \simeq m_3 \simeq \sqrt{\Delta m_a^2}$ and $p_0 = m_2^0/m_3^0 \simeq p \simeq \sqrt{\Delta m_s^2/\Delta m_a^2}$, we find

$$|\epsilon_1 - \epsilon_3 g| \simeq \sqrt{\frac{\Delta m_s^2}{\Delta m_a^2}}\ \Theta \simeq 0. \tag{30}$$

2. The NH case in the regions of $m_2 \simeq m_1$ ($p > 0.4$).
   This case occurs when the neutrinoless double beta decay is observed in the phase-II experiments. By taking the limit of $m_i = m_i^0$ and $m_2^0 = m_1^0$, the consistency condition can be rewritten as

$$\left| \mathrm{Re}(e^{-\frac{i}{2}(\alpha_0+\beta_0)} (\epsilon_1 - \epsilon_3 g)) \right| \simeq \frac{(1-p^2)}{2p} \left(\frac{\Delta m_s^2}{\Delta m_a^2} \right)\ \Theta \simeq 0. \tag{31}$$

   Note that $\beta_0 \simeq \beta$ and $\alpha_0 \simeq \alpha$.

3. The IH case.
   In the case of IH, $\mu = m_2^0$ and

$$k_1 = \frac{m_1^0}{m_2^0} e^{i\alpha_0}, \quad k_2 = e^{i\beta_0}, \quad k_3 = \frac{m_3^0}{m_2^0}. \tag{32}$$

   Since m_2 is always quasi-degenerated with m_1, the consistent condition turns out

$$\left| \mathrm{Re}\left(e^{-\frac{i}{2}(\alpha_0+\beta_0)} (\epsilon_1 - \epsilon_3 g) \right) \right| \simeq \frac{(1-(1/p)^2)}{2} \left(\frac{\Delta m_s^2}{\Delta m_a^2} \right)\ \Theta \simeq 0. \tag{33}$$

In all the cases, the key ingredient is $\epsilon_1 - \epsilon_3 g$, and the consistency conditions force ϵ_1 to be of the order of $\epsilon_{2,3}^2$. In other words, one needs to tune ϵ_1 to cancel out $\epsilon_3 g$. As we shall demonstrate in the next section, this causes unnatural parameter-tuning in some cases.

5 Tri-bi-maximal mixing case

We here choose the Tri-Bi-Maximal (TBM) mixing [14, 15, 16] matrix V_{TBM} as V_0,

$$V_{\mathrm{TBM}} = \begin{pmatrix} \sqrt{\frac{2}{3}} & \frac{1}{\sqrt{3}} & 0 \\ -\frac{1}{\sqrt{6}} & \frac{1}{\sqrt{3}} & \frac{1}{\sqrt{2}} \\ \frac{1}{\sqrt{6}} & -\frac{1}{\sqrt{3}} & \frac{1}{\sqrt{2}} \end{pmatrix}. \tag{34}$$

In this case, the full mixing matrix after perturbation is obtained as

$$
\begin{aligned}
V &= V_{\rm TBM} V_1 V_2 \\
&\simeq \begin{pmatrix}
\sqrt{\frac{2}{3}}\left(1-\frac{1}{\sqrt{2}}\mathcal{S}e^{-i\kappa}\right) & \frac{1}{\sqrt{3}}\left(1+\sqrt{2}\mathcal{S}e^{i\kappa}\right) & \frac{1}{\sqrt{3}}(\sqrt{2}f+g)^* \\
-\frac{1}{\sqrt{6}}(1+\sqrt{3}f-\sqrt{2}\mathcal{S}e^{-i\kappa}) & \frac{1}{\sqrt{3}}\left(1-\sqrt{\frac{3}{2}}g-\frac{1}{\sqrt{2}}\mathcal{S}e^{i\kappa}\right) & \frac{1}{\sqrt{2}}\left(1+\frac{1}{\sqrt{3}}(-f+\sqrt{2}g)^*\right) \\
\frac{1}{\sqrt{6}}(1-\sqrt{3}f+\sqrt{2}\mathcal{S}e^{-i\kappa}) & -\frac{1}{\sqrt{3}}\left(c_2+\sqrt{\frac{3}{2}}g-\frac{1}{\sqrt{2}}\mathcal{S}e^{i\kappa}\right) & \frac{1}{\sqrt{2}}\left(1-\frac{1}{\sqrt{3}}(-f+\sqrt{2}g)^*\right)
\end{pmatrix},
\end{aligned}
$$

up to the first order of f, g, and $\mathcal{S}$. The mixing angles are derived as

$$
\begin{aligned}
&\sin\theta_{13}\, e^{-i\delta} \simeq V_{13} = \frac{1}{\sqrt{3}}(\sqrt{2}f+g)^*, \\
&\sin^2\theta_{23} \simeq |V_{23}|^2 \simeq \frac{1}{2}\left(1+\frac{2}{\sqrt{3}}{\rm Re}[-f+\sqrt{2}g]\right),
\end{aligned}
\tag{35}
$$

and

$$
\sin^2\theta_{12} = \frac{|V_{12}|^2}{c_{13}^2} \simeq \frac{1}{3}\left(1+2\sqrt{2}\mathcal{S}\cos\kappa+\mathcal{S}^2-\frac{2}{3}\left\{|g|^2-|f|^2-\sqrt{2}{\rm Re}[fg^*]\right\}\right), \tag{36}
$$

where κ is defined in Eq. (19). We have taken into account the second order terms of f and g for $\sin^2\theta_{12}$ as they could be the main contributor depending on the sizes of $\cos\kappa$ and $\mathcal{S}$. Note that the orders of $|f|$ and $|g|$ are constrained by $\sin\theta_{13}$ and $\sin\theta_{23}$, and their contributions to $\sin^2\theta_{12}$ are at most ± 0.01; in contrast, they are crucial when evaluating $\mathcal{S}$ as we outlined in Sect. 3.

According to the latest global analysis by Capozzi et. al. [8], the allowed 2σ (3σ) range is $0.275(0.259) \leq \sin^2\theta_{12} \leq 0.342(0.359)$, which places

$$
F-0.062(-0.079) \;\leq\; \mathcal{S}\left[\cos\kappa+\frac{1}{2\sqrt{2}}\mathcal{S}\right] \;\leq\; F+0.009(0.027), \tag{37}
$$

where $F=\sqrt{2}/6\left\{|g|^2-|f|^2-\sqrt{2}{\rm Re}[fg^*]\right\}$. The angle $\mathcal{S}\simeq\Theta$ is much smaller than the first order term as long as $\cos\kappa$ is not very small. Even in the case $\cos\kappa=0$, $\mathcal{S}$ is the first order term.

In below, we examine the behavior of $\cos\kappa$ for the three cases.

1. The NH case in the regions of $m_2 \gg m_1$.
   We find $a^*c+bc^* \simeq p_0 e^{i\beta_0}(\epsilon_1-\epsilon_3 g)^*$, so that

   $$\kappa = \beta_0 - \arg(\epsilon_1-\epsilon_3 g). \tag{38}$$

   It may be worthwhile to note that β_0 is almost equal to the Majorana CP violating phase β because the phase of V_{12} is suppressed and phases of V_{23} and V_{33} are absorbed by charged lepton fields.

2. The NH case in the regions of $m_2 \simeq m_1$.
   Since $m_1^0 \simeq m_2^0$, we find

   $$a^*c+bc^* \simeq 2p_0 e^{-\frac{i}{2}(\alpha_0-\beta_0)}{\rm Re}\left[e^{-\frac{i}{2}(\alpha_0+\beta_0)}(\epsilon_1-\epsilon_3 g)\right], \tag{39}$$

   and thus

   $$\kappa = -\frac{1}{2}(\alpha_0-\beta_0). \tag{40}$$

   Because $\alpha_0 \simeq \alpha$ and $\beta_0 \simeq \beta$, one readily notices that

   $$
   \begin{aligned}
   &\cos\kappa \simeq \pm 1 \quad \text{when} \quad \alpha=\beta \;\text{ or }\; \alpha=\beta+2\pi, \\
   &\cos\kappa \simeq 0 \quad \text{when} \quad \alpha=\beta\pm\pi.
   \end{aligned}
   \tag{41}
   $$

Namely, the former happens in the case of the constructing interference of the Majorana phases, while the latter is the case of the destructive interference. It should be noted that for $\cos\kappa = -1$, the correction decreases $\sin\theta_{12}$ because we choose $\mathcal{S} \geq 0$, while for $\cos\kappa = 1$ and $\cos\kappa = 0$, the correction increases it. The present tendency seems to disfavor the $\cos\kappa = 1$ and $\cos\kappa = 0$ cases.

3. The IH case.
   In this case, we find

$$a^*c + bc^* \simeq 2e^{-\frac{i}{2}(\alpha_0-\beta_0)}\mathrm{Re}\left[e^{-\frac{i}{2}(\alpha_0+\beta_0)}(\epsilon_1 - \epsilon_3 g)\right], \tag{42}$$

   and thus

$$\kappa = -\frac{1}{2}(\alpha_0 - \beta_0). \tag{43}$$

   Note that α_0 and β_0 are not necessarily equal to the physical Majorana phases when $m_3 \simeq 0$, but $\alpha_0 - \beta_0 \simeq \alpha - \beta$ still holds[5]. Therefore, like the previous case, $\cos\kappa \simeq \pm 1$ and $\cos\kappa \simeq 0$ occur in the constructive and destructive interference cases, respectively.

5.1 Parameter tuning

Let us roughly estimate how strong the parameter-tuning required by the consistency condition is. Taking the limits of $\cos\kappa = -1$ and $\cos\kappa = 0$, we place $|\sin^2\theta_{12} - 1/3| \leq 0.025$. This number corresponds to the best-fit-value and 3σ-upper-bound [8] for $\cos\kappa = -1$ and 0, giving rise to $\Theta \leq 0.027$ and 0.28, respectively. Also, we will use $\Delta m_s^2/\Delta m_a^2 = 0.031$ and ignore the corrections from the second order terms of f and g.

1. The NH case in the regions of $m_2 \gg m_1$.
   The consistency condition is given in Eq. (30). For $\cos\kappa = -1$, we find

$$\left|\frac{\epsilon_1}{\epsilon_3 g} - 1\right| < 0.12. \tag{44}$$

   For $\cos\kappa = 0$, the parameter-tuning is not so serious. We have substituted $|\epsilon_3 g| \simeq |fg| = 0.04$ in view of $\sin^2\theta_{13}^{\mathrm{best}} \simeq 0.023$ [8].

2. The NH case in the regions of $m_2 \simeq m_1$.
   We simplify the left-hand side of Eq. (31) as $|\epsilon_1 - \epsilon_3 g|$. For $\cos\kappa = -1$ and $\cos\kappa = 0$, we find

$$\left|\frac{\epsilon_1}{\epsilon_3 g} - 1\right| < 0.037(0.023) \ \text{ for } \ p = 0.4(0.8), \tag{45}$$

   and

$$\left|\frac{\epsilon_1}{\epsilon_3 g} - 1\right| < 0.37(0.24) \ \text{ for } \ p = 0.4(0.8), \tag{46}$$

   respectively, where $p = m_2/m_3$, and $|\epsilon_3 g| \simeq (1-p)|fg| = 0.04(1-p)$ is assumed.

3. The IH case.
   We simplify the left-hand side of Eq. (33) as $|\epsilon_1 - \epsilon_3 g|$. For $\cos\kappa = -1$ and $\cos\kappa = 0$, we find

$$\left|\frac{\epsilon_1}{\epsilon_3 g} - 1\right| < 0.010(0.019) \ \text{ for } \ 1/p = 0(0.8), \tag{47}$$

[5] Also, if $\alpha_0 \simeq \beta_0$, then $\alpha \simeq \beta$.

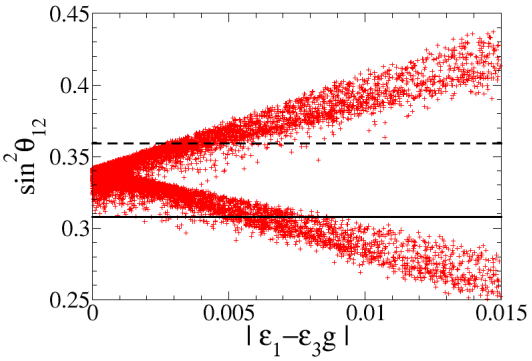

Figure 2: The scatter plot of $\sin^2\theta_{12}$ for the NH in the case of $m_1 = 0$ and $\cos\kappa = \pm 1$. The horizontal dashed- and solid-lines display the 3σ-upper-bound and best-fit-value, respectively.

and

$$\left|\frac{\epsilon_1}{\epsilon_3 g} - 1\right| < 0.11(0.19) \quad \text{for} \quad 1/p = 0(0.8), \tag{48}$$

respectively, where $|\epsilon_3 g| \simeq (1 - 1/p)|fg| = 0.04(1 - 1/p)$ is assumed.

As demonstrated above, from a few % to several tens of % tuning is required between ϵ_1 and $\epsilon_3 g$. In particular, somewhat strong parameter-tuning may be necessary in the case of $m_2 \simeq m_1$ with $\beta \simeq \alpha$.

5.2 Validity of consistency conditions

We numerically diagonalize the mass matrix and check the validity of the consistency conditions Eqs. (30), (31) and (33). In the numerical calculations, we place the 1σ error bounds for Δm_s^2, Δm_a^2, $\sin^2\theta_{13}$, and $\sin^2\theta_{23}$ from Ref. [8]:

$$\begin{aligned}
&\Delta m_s^2 = (7.32 - 7.80) \times 10^{-5} \ \text{eV}^2, \quad \Delta m_a^2 = \begin{cases} (2.38 - 2.52) \times 10^{-3} \ \text{eV}^2 \\ (2.33 - 2.47) \times 10^{-3} \ \text{eV}^2 \end{cases}, \\
&\sin^2\theta_{13} = \begin{cases} (2.16 - 2.56) \times 10^{-2} \\ (2.18 - 2.60) \times 10^{-2} \end{cases}, \quad \sin^2\theta_{23} = \begin{cases} (3.98 - 4.54) \times 10^{-1} & \text{for NH} \\ (4.08 - 4.96) \times 10^{-1} & \text{for NH} \end{cases}.
\end{aligned} \tag{49}$$

In Figs. 2 and 3, we plot $\sin^2\theta_{12}$ as a function of the left-hand side of the consistency condition for Eqs. (30) and (31). The figures for Eq. (33) are almost the same as Fig. 3. In Fig. 2, $m_1 = 0$ and $\cos\kappa = \pm 1$ are assumed. The left and right panels in Fig. 3 are the cases of the constructive interference ($\cos\kappa = \pm 1$) and destructive interference ($\cos\kappa = 0$), respectively, for $p = 0.4 - 0.8$. All the CP phases are varied from 0 to 2π, and $|\epsilon_2|$ and $|\epsilon_3|$ run from 0.00 to 0.25.

From the figures, one can observe a trend that $\sin^2\theta_{12}$ approaches to its TBM value as the consistency conditions are satisfied. In the left panel of Fig. 3, however, $\sin^2\theta_{12}$ departs from the TBM value even if the x-axis is zero. This is due to the failure of the approximations made above Eq. (23), and this indicates that one needs to take into account next higher-order terms and tune $\epsilon_1 - \epsilon_3 g$ to cancel out them. The resulting condition would be very complex and require much more delicate parameter-tuning. Hence, we do not go into its detail here. In the next section, we shall invent several models where the consistency conditions Eqs. (31) and (33) work very well.

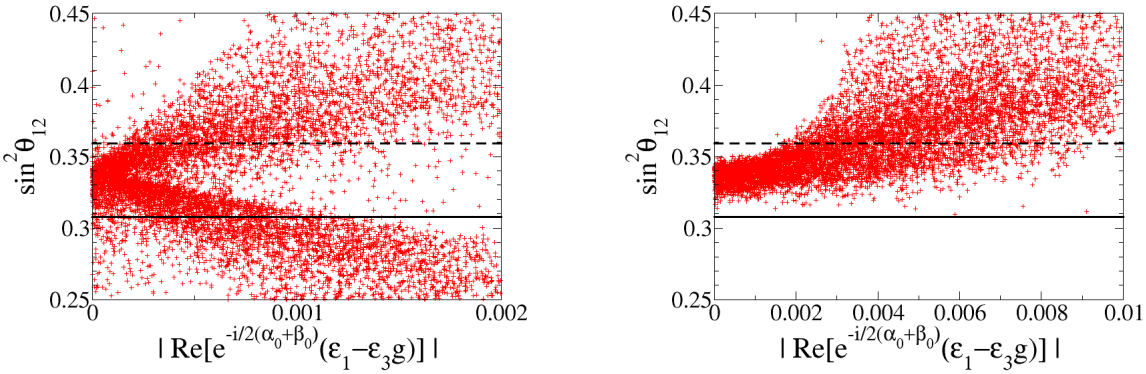

Figure 3: The scatter plots of $\sin^2\theta_{12}$ for the NH in the mass regions of $m_2 \simeq m_1$ ($p = 0.4 - 0.8$), with $\cos\kappa = \pm 1$ (left panel) and $\cos\kappa = 0$ (right panel). The horizontal dashed- and solid-lines display the 3σ-upper-bound and best-fit-value, respectively.

6 Applications to models

As we demonstrated in the previous section, the consistency conditions could be satisfied by tuning ϵ_1. However, it may be difficult to explain such parameter-tuning by model-building. Furthermore, in some cases, the consistency conditions fail to keep $\sin\theta_{12}$ within experimentally-realistic ranges. In this section, we consider two other possibilities by postulating $\epsilon_1 = 0$: (1) adjusting either $|\epsilon_2|$ or $|\epsilon_3|$ to be very small, and (2) adjusting CP phases. In the models proposed below, the consistency conditions work very well. Moreover, they seem attractive from model-building and/or phenomenological points of view. For definition, we again employ the TBM mixing as V_0.

6.1 Adjusting $|\epsilon_2|$ or $|\epsilon_3|$

The consistency conditions Eqs. (30), (31), and (33) can be satisfied by making either $|\epsilon_2|$ or $|\epsilon_3|$ vanishing when $|\epsilon_1| = 0$. The following arguments are independent on the neutrino masses and Majorana phases.

- $|\epsilon_2| = 0$ ($g = 0$) case.
  In this case, the mixing matrix turns out to be the so-called tri-maximal mixing [17]:

$$V = V_{\rm TBM} V_1(\epsilon_2 = 0) \simeq \begin{pmatrix} \sqrt{\frac{2}{3}} & \frac{1}{\sqrt{3}} & \sqrt{\frac{2}{3}} f^* \\ -\frac{1}{\sqrt{6}}(1+\sqrt{3}f) & \frac{1}{\sqrt{3}} & \frac{1}{\sqrt{2}}\left(1 - \frac{1}{\sqrt{3}} f^*\right) \\ \frac{1}{\sqrt{6}}(1-\sqrt{3}f) & -\frac{1}{\sqrt{3}} & \frac{1}{\sqrt{2}}\left(1 + \frac{1}{\sqrt{3}} f^*\right) \end{pmatrix}. \tag{50}$$

  Its mixing properties have been extensively studied by many authors, so that we refrain from going into details. See, for instance, Refs. [18, 19, 20, 21] for the behavior of $\sin^2\theta_{12}$ and the others. Nevertheless, several comments are in order. (1) The higher-order term of f included in Eq. (36) slightly increases $\sin^2\theta_{12}$; thus $\sin^2\theta_{12} > 1/3$ is predicted. (2) The model have a prediction among $\sin\theta_{13}$, $\sin\theta_{23}$, and the Dirac phase δ:

$$\cos\delta = \frac{\sqrt{2}}{\sin\theta_{13}}\left(\frac{1}{2} - \sin^2\theta_{23}\right). \tag{51}$$

  Note that when $\sin\theta_{23} = 1/\sqrt{2}$, then $\delta = \pi/2$ or $3\pi/2$.

It may be interesting to note that the corresponding mass matrix preserves a Z_2 symmetry even after adding the perturbation terms. It is well known that the TBM mixing can be derived from the mass matrix invariant under the following Z_2 symmetries [22, 23, 24] (see also Ref. [25]):

$$G_1^{\rm TBM} = \begin{pmatrix} 1 & 0 & 0 \\ 0 & 0 & -1 \\ 0 & -1 & 0 \end{pmatrix}, \quad G_2^{\rm TBM} = \frac{1}{3}\begin{pmatrix} 1 & -2 & 2 \\ -2 & 1 & 2 \\ 2 & 2 & 1 \end{pmatrix}, \tag{52}$$

in the flavor basis. In the case of $|\epsilon_1| = |\epsilon_2| = 0$, $G_2^{\rm TBM}$ remains unbroken. This often happens in a class of the A_4 flavor model [26, 27, 28] because A_4 does not include $G_1^{\rm TBM}$.

It should also be noted that the difficulty to keep θ_{12} around the TBM value, while reproducing a large θ_{13}, in the A_4 flavor model was pointed out in Refs. [29, 30, 31]. They arrived at the same solution, $\epsilon_1 = \epsilon_2 = 0$, and Eq. (51).

- $|\epsilon_3| = 0$ ($f = 0$) case.
  In this case, the mixing matrix takes the form of

$$V = V_{\rm TBM} V_1(\epsilon_3 = 0) \simeq \begin{pmatrix} \sqrt{\frac{2}{3}} & \frac{1}{\sqrt{3}} & \frac{1}{\sqrt{3}} g^* \\ -\frac{1}{\sqrt{6}} & \frac{1}{\sqrt{3}}\left(1 - \sqrt{\frac{3}{2}} g\right) & \frac{1}{\sqrt{2}}\left(1 + \sqrt{\frac{2}{3}} g^*\right) \\ \frac{1}{\sqrt{6}} & -\frac{1}{\sqrt{3}}\left(1 + \sqrt{\frac{3}{2}} g\right) & \frac{1}{\sqrt{2}}\left(1 - \sqrt{\frac{2}{3}} g^*\right) \end{pmatrix}. \tag{53}$$

  This mixing patten is also analyzed in Refs. [18, 20, 21]. In contrast to the tri-maximal mixing, the higher-order term of g included in Eq. (36) slightly decreases $\sin^2\theta_{12}$; thus $\sin^2\theta_{12} < 1/3$ is predicted. The model prediction among $\sin\theta_{13}$, $\sin\theta_{23}$, and δ is

$$\cos\delta = \frac{1}{\sqrt{2}\sin\theta_{13}}\left(\sin^2\theta_{23} - \frac{1}{2}\right). \tag{54}$$

  As is the case of the tri-maximal mixing, the mass matrix preserves $G_1^{\rm TBM} G_2^{\rm TBM}$ in the flavor basis.

6.2 Adjusting phases

We restrict ourselves to the case of $m_2 \simeq m_1$ (as well as $\epsilon_1 = 0$) and parametrize ϵ_3 and ϵ_2 as

$$\epsilon_3 = E_3 e^{i\rho_3}, \quad \epsilon_2 = E_2 e^{i\rho_2}, \tag{55}$$

where $E_3 = |\epsilon_3|$ and $E_2 = \pm|\epsilon_2|$. Then, the consistency conditions Eqs. (31) and (33) are expressed as

$$\left| \frac{E_2 E_3}{k_3^2 - |k_2|^2} \left[k_3 \cos(\alpha_0 - \rho_2 - \rho_3) + |k_2| \cos(\rho_2 - \rho_3) \right] \right| \simeq 0, \tag{56}$$

for the constructive interference, while

$$\left| \frac{E_2 E_3}{k_3^2 - |k_2|^2} \left[k_3 \sin(\alpha_0 - \rho_2 - \rho_3) - |k_2| \sin(\rho_2 - \rho_3) \right] \right| \simeq 0, \tag{57}$$

for the destructive interference. Here, $k_3 = 1$ and $|k_2| = m_2^0/m_3^0 = p_0$ for the NH case, while $k_3 = m_3^0/m_2^0 = 1/p_0$ and $|k_2| = 1$ for the IH case. Suppose neither $E_3 = 0$ nor $E_2 = 0$, these conditions can be satisfied by adjusting the CP phases.

- The NH case with the constructive interference and $\rho_2 = \rho_3 \equiv \rho$.
  In this case, Eq. (56) provides us with

$$|\cos(2\rho - \alpha_0) + p_0| \simeq 0. \tag{58}$$

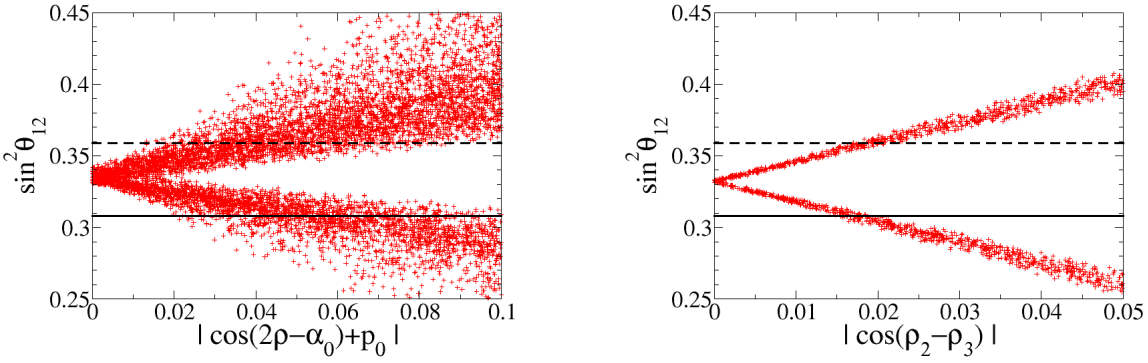

Figure 4: Left panel: the scatter plot of $\sin^2\theta_{12}$ for the NH in the mass regions of $m_2 \simeq m_1$ ($p = 0.4 - 0.8$), with $\cos\kappa = \pm 1$ and $\rho_2 = \rho_3$. Right panel: the scatter plot of $\sin^2\theta_{12}$ for the IH case with $m_3 \simeq 0$ and $\cos\kappa = \pm 1$. The horizontal dashed- and solid-lines display the 3σ-upper-bound and best-fit-value, respectively.

In the left panel of Fig. 4, we numerically diagonalize the mass matrix and plot $\sin^2\theta_{12}$ as a function $|\cos(\alpha_0 - 2\rho) + p_0|$ for $E_2 > 0$. It can be seen that $\sin^2\theta_{12}$ approaches to the TBM value as $|\cos(\alpha_0 - 2\rho) + p_0|$ gets close to zero.

By substituting $\cos(2\rho - \alpha_0) = -p_0$ into f and g in Eq. (24), we find

$$\begin{aligned} f &= \frac{E_3}{\sqrt{1-p_0^2}} e^{i(\alpha_0 - \rho - \pi/2)}, \\ g &= \frac{E_2}{\sqrt{1-p_0^2}} e^{i(\alpha_0 - \rho - \pi/2)}. \end{aligned} \tag{59}$$

In turn, from the first identity of Eq. (35), it is found that ρ is given by the Dirac and Majorana phases as

$$\rho = \alpha_0 - \delta \mp \pi/2, \tag{60}$$

where $\pm$ stems from the sign of V_{13}, yielding

$$\cos(\alpha_0 - 2\delta) \simeq p_0. \tag{61}$$

Since $p_0 \simeq p$ and $\alpha_0 \simeq \alpha$, this is the relation among observables and the prediction of this model. Furthermore, $\sin\theta_{13}$ and $\sin\theta_{23}$ are expressed as

$$\begin{aligned} |\sqrt{2}E_3 + E_2| &= \sqrt{3(1-p_0^2)}\sin\theta_{13}, \\ |-E_3 + \sqrt{2}E_2| &= \sqrt{6(1-p_0^2)}\left|\frac{\sin\theta_{23} - 1/\sqrt{2}}{\cos\delta}\right|. \end{aligned} \tag{62}$$

Let us emphasize two more-simplified models. (1) If both ϵ_3 and ϵ_2 are real, i.e., $\rho = 0$, the Majorana CP phase α is directly related to the Dirac CP phase δ via

$$\alpha = \delta \pm \pi/2, \tag{63}$$

and also δ is related to p as

$$p = \mp \sin\delta. \tag{64}$$

(2) If $\epsilon_3 = \sqrt{2}\epsilon_2$ (thus, $E_3 = \sqrt{2}E_2$) the model predicts the maximal θ_{23}. This prediction is favored by the latest data of ν_μ-disappearance reported by the T2K experiment [32].

- The IH case.
  The same situation, $\rho_2 = \rho_3$ and $\beta_0 = \alpha_0$, cannot be applied for the IH case because it leads to

$$\left| \frac{1}{p_0} \cos\left(2\rho - \alpha_0\right) + 1 \right| \simeq 0, \tag{65}$$

  which cannot be satisfied because $(1/p_0) < 1$[6]. This seems to be a quite strong constraint for model-building.

  Instead, it may be interesting to consider the case of $m_3 \simeq 0$, since a massless active neutrino can be realized by considering two-right-handed-neutrino seesaw scenarios [33, 34, 35, 36]. In this case, the consistency conditions become

$$|\cos(\rho_2 - \rho_3)| \ll 1 \quad \text{or} \quad \rho_2 - \rho_3 \simeq \frac{\pi}{2} \mod \pi \tag{66}$$

  for the constructive interference, while

$$|\sin(\rho_2 - \rho_3)| \ll 1 \quad \text{or} \quad \rho_2 - \rho_3 \simeq 0 \mod \pi \tag{67}$$

  for the destructive interference. As can be seen, they suggest correlations between ρ_3 and ρ_2. Conversely, it can be said that one can naturally satisfy the consistency conditions once the phase correlations are explained by model-building. The scatter plot of $\sin^2\theta_{12}$ for the constructive interference case is displayed in the right panel of Fig. 4.

7 The concluding remarks

We have seen that some correspondences between the constraint on input parameters and the output constraints on experimental observables. It is amazing that this kind of correlation is observed analytically as we have illustrated. The feature we saw here is a general one for models where we start from the neutrino mass matrix which reproduce experimental data well and reproduce the data by adding small perturbation terms in the presence of the degeneracy between m_2 and m_1. Our method will be useful for model building.

References

[1] W. Rodejohann, Int. J. Mod. Phys. E**20**, 1833 (2011).

[2] S. M. Bilenky and C. Giunti, Mod. Phys. Lett. A**27**, 1230015 (2012).

[3] F. Simkovic, S. M. Bilenky, A. Faessler, and Th. Gutsche, Phys. Rev. D**87**, 073002 (2013).

[4] N. Haba and R. Takahashi, Acta Phys. Polon. B**45**, 61 (2014).

[5] H. Minakata, H. Nunokawa, and A. A. Quiroga, arXiv:1402.6014 [hep-ph].

[6] H. V. Klapdor-Kleingrothaus, H. Päs, and A.Y. Smirnov, Phys. Rev. D**63**, 073005 (2001).

[7] S. Pascoli and S. T. Petcov, Phys. Lett. B**544**, 239 (2002).

[8] F. Capozzi et al, arXiv:1312.2878 [hep-ph].

[6] It is possible to consider $\rho_2 = \rho_3$ for the destructive interference case.

[9] EXO Collaboration, Phys. Rev. Lett. **109**, 032505 (2012).

[10] KamLAND-Zen Collaboration, Phys. Rev. Lett. **110**, 062502 (2013).

[11] Planck Collaboration, arXiv:1303.5076 [astro-ph.CO].

[12] M. Doi, T. Kotani, H. Nishiura, K. Okuda, and E. Takasugi, Phys. Lett. B**102**, 323 (1981).

[13] M. Doi, T. Kotani, H. Nishiura, K. Okuda, and E. Takasugi, Prog. Theor. Phys. **66**, 1739 (1981); Erratum-ibid. **68**, 347 (1982).

[14] P. F. Harrison, D. H. Perkins, and W. G. Scott, Phys. Lett. B **530**, 167 (2002).

[15] Z. Z. Xing, Phys. Lett. B **533**, 85 (2002).

[16] P. F. Harrison and W. G. Scott, Phys. Lett. B **535**, 163 (2002).

[17] W. Grimus and L. Lavoura, J. High Energy Phys. **0809**, 106 (2008).

[18] C. H. Albright and W. Rodejohann, Eur. Phys. J. C**62**, 599 (2009).

[19] Y. Shimizu, M. Tanimoto and A. Watanabe, Prog. Theor. Phys. **126**, 81 (2011).

[20] X. G. He and A. Zee, Phys. Rev. D**84**, 053004 (2011).

[21] L. J. Hall and G. G. Ross, J. High Energy Phys. **1311**, 091 (2013).

[22] C. S. Lam, Phys. Lett. B**656**, 193 (2007).

[23] C. S. Lam, Phys. Rev. Lett. **101**, 121602 (2008).

[24] C.S. Lam, Phys. Rev. D**78**, 073015 (2008).

[25] W. Grimus, L. Lavoura and P. O. Ludl, J. Phys. G**36**, 115007 (2009).

[26] G. Altarelli and F. Feruglio, Nucl. Phys. B **720**, 64 (2005).

[27] G. Altarelli and F. Feruglio, Nucl. Phys. B**741**, 215 (2006).

[28] E. Ma, Phys. Rev. D**73**, 057304 (2006).

[29] Y. Lin, Nucl. Phys. B**824**, 95 (2010).

[30] G. Altarelli, F. Feruglio, L. Merlo, and E. Stamou, J. High Energy Phys. **1208**, 021 (2012).

[31] G. Altarelli, F. Feruglio, and L. Merlo, Fortsch. Phys. **61**, 507 (2013).

[32] T2K Collaboration, Phys. Rev. Lett. **111**, 211803 (2013).

[33] P. H. Frampton, S. L. Glashow, and T. Yanagida, Phys. Lett. B **548**, 119 (2002).

[34] T. Endoh, S. Kaneko, S. K. Kang, T. Morozumi, and M. Tanimoto, Phys. Rev. Lett. **89**, 231601 (2002).

[35] T. Kitabayashi, Phys. Rev. D **76**, 033002 (2007); Prog. Theor. Phys. **120**, 443 (2008).

[36] B. Brahmachari and N. Okada, Phys. Lett. B **660**, 508 (2008).